Wind Field Variations in the Tropical Pacific Ocean from Satellite Scatterometer Data

HO Chung-ru [1], ZHENG Zhe-wen [1], LIN Chun-yi [1], KUO Nan-jung [1], TSAO Chih-chung [2]

[1]Department of Marine Environmental Informatics, National Taiwan Ocean University, Keelung, Taiwan, China
E-mail: chungru.ho@gmail.com
[2]Department of Social Studies Education, National Taipei University of Education, Taipei, Taiwan, China

Abstract
Satellite scatterometers have provided an opportunity to monitor wind fields in the world oceans. The sea surface wind stress data from ERS-1/2 and QuikSCAT scatterometers from 1993 to 2007 has been used to study the variation in the tropical Pacific Ocean by vector empirical orthogonal function (VEOF) method. The first VEOF mode shows an increase trend of planetary wind stress. The significantly increasing period is found from 1999 to 2000 when is the data transferred from ERS-2 to QuikSCAT. The consistence between ERS-1/2 and QuikSCAT winds during the overlap period from 1999 to 2000 is examined. The results show that there is a significant difference between the two datasets. The ERS-1/2 data is then adjusted to fit the wind data from QuikSCAT by least squares method. VEOF is then applied to the wind dataset again and no increasing trend is found in the first VEOF mode which is related to the trade winds. The second VEOF mode indicates the seasonal variation which is related to the East Asia monsoon. After removing the annual signal, the anomaly wind data are decomposed by VEOF again. The first mode shows the interannual variability which is highly related to El Niño/La Niña events.

Keywords
satellite scatterometer, wind stress, vector empirical orthogonal function, tropical ocean

I. INTRODUCTION

The wind system over the tropical Pacific Ocean including the East Asia monsoon and the trade winds plays a major role in the regional climate variation. Previous studies have demonstrated that the East Asia monsoon might influence the rainfall in the East Asia continent(Lau K M, et al., 2000; Lau K M, et al., 2002; Huang R H, et al., 2002; Zhu C W, et al., 2003; Qian J H, et al., 2004). The major interannual variability, El Nino/La Nina, is believed to be related to the variation of wind system in the tropical Pacific. Kawamura(1998) showed that there is a high correlation between Asian summer monsoon and ENSO due to anomalous sea surface temperature in the tropical oceans. Pan et al.(2003) analyzed the wind data of northwestern Pacific and found that the wind field is related to Southern Oscillation Index (SOI), but has a half-year lag with respect to the SOI. Besides the relationship between tropical Pacific wind fields and ENSO, the long-term variation of wind field has also been investigated. Inoue and Bigg(Inoue M, et al., 1995) analyzed COADS (Comprehensive Ocean-Atmosphere Data Set) sea-level pressure and wind observations and pointed out the trade winds gained strength over the eastern/central equatorial Pacific during the period 1950–1979. Clarke and Lebedev(Clarke A. J., et al., 1999) also analyzed COADS and suggested the surface pressure difference between eastern and western equatorial Pacific can be used to monitor wind stress of trade wind. The intensity of wind stress over the equatorial Pacific is fluctuated but it has weakened from the end of 1960s. Most previous studies used in-situ measurements to study the variation of wind. However because of the rarity and irregularly special distribution of in-situ measurements, the bias of statistics for wind field study is a key problem. In this study, we will use satellite data which are operationally achieved and uniform distributed in space to study the relationship between the variation of wind stress and ENSO event, as well as the long-term trend of wind stress over the tropical Pacific Ocean.

II. DATA AND METHODOLOGY

A. Surface wind data

The sea surface wind data which were derived from the scatterometers of European Remote Sensing (ERS) satellite -1/2 and NASA's Quick Scatterometer (QuikSCAT) were acquired from French Research Institute for Exploitation of the Sea (IFREMER). The period of this dataset was from January 1993 to May 2001 for ERS-1/2 and was from August 1999 to August 2007 for QuikSCAT with an overlap period from August 1999 to May 2001, a total of 22 months. ERS-1 and ERS-2 were launched on the 17th July 1991 and on the 21st April 1995, respectively. Both satellites carried the same type of Active Microwave Instrument (AMI) operated as synthetic aperture radar or as a wind scatterometer. The spatial resolutions for ERS and QuikSCAT wind data are 1° and 0.5°, respectively. To assemble a longer time series of wind stress data set with same spatial resolution, the ERS wind data were interpolated linearly into 0.5° × 0.5° and merged with QuikSCAT wind data. During the overlap period, both datasets were combined directly by replacing ERS wind forcing with QuikSCAT wind forcing. The monthly means of the merged

1082-4006/08/14(02)-120$5.00

wind stress with 0.5° spatial resolutions serves as the baseline for this study.

B. Methodology

In order to examine the spatial and temporal variability of the wind stress, we performed a vector empirical orthogonal function (VEOF) analysis(Pan J, et al., 2003). The EOF analysis is a statistical method, which can extract a small number of principal components accounting for the most dominant variation of the original data set(Lagerloef G S E, et al., 1988) and has proven to be a useful tool for resolving physical processes in atmosphere and oceans (Kelly K A, 1988). The original data set $D(x, y, t)$ at longitude, x, latitude, y, and time, t, can be expressed as a matrix **D** with dimension $m \times n$, where M is the number of spatially distributed points and N is the number of observation over time. The EOF analysis can be used to decompose **D** into two orthogonal matrices as **D=AB**, where **A** is a matrix of $m \times I$, **B** is a matrix of $I \times n$, and I is the number of nonzero EOF modes. The original data set $D(x, y, t)$ can be expressed as a linear combination of the product of the spatial function $A_n(x, y)$ and the time-varying function $B_n(t)$, that is

$$D(x, y, t) = \sum_n A_n(x, y) B_n(t) \quad (1)$$

$A_n(x, y)$ is the distribution of the spatial patterns of the variance of the nth mode and $B_n(t)$ is the modulated function of the nth mode in the time domain. The VEOF method applies the EOF decomposition to the wind vector data as suggested by(Hardy D M, et al., 1978). The $M \times N$ matrix of u component **U** and v component **V** of wind stress $\mathbf{W}(x, y, t)$ are merged to form a new $2M \times N$ matrix **S** as

$$\mathbf{S} = \begin{bmatrix} \mathbf{U} \\ \mathbf{V} \end{bmatrix} \quad (2)$$

The singular value decomposition (SVD) is then applied to the new matrix. The decomposition is given as

$$\mathbf{W}(x, y, t) = \sum_n C_n(x, y) B_n(t) \quad (3)$$

where $C_n(x, y)$ is the nth spatial VEOF and $B_n(t)$ is the nth temporal VEOF.

III. RESULTS AND DISCUSSIONS

A. Comparison between ERS-2 and QuikSCAT

We applied the VEOF analysis to the combined wind stress dataset of ERS-1/2 and QuikSCAT from January 1993 to August 2007. The first VEOF mode shows the planetary wind stress in spatial domain with an obvious increase of amplitude around 2000 in temporal domain (Figure 1). It is very interesting to examine whether the wind stress increasing is true or not. We averaged the wind stress in u- and v-components in the study area during the overlap period of ERS-2 and QuikSCAT from January to December 2000(Figure 2). One can see that the magnitudes derived from ERS-2 both in u- and v-components are smaller

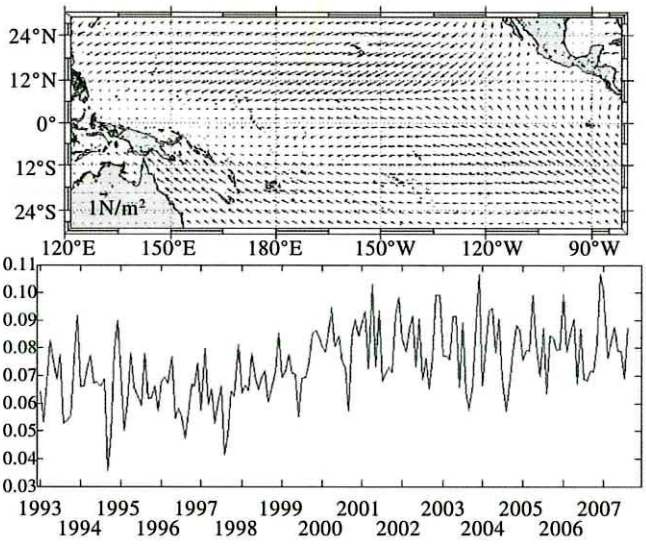

Figure 1. The first VEOF of the tropical Pacific surface wind stress with the spatial mode (upper) in which the arrows represent wins stress directions, and the temporal mode

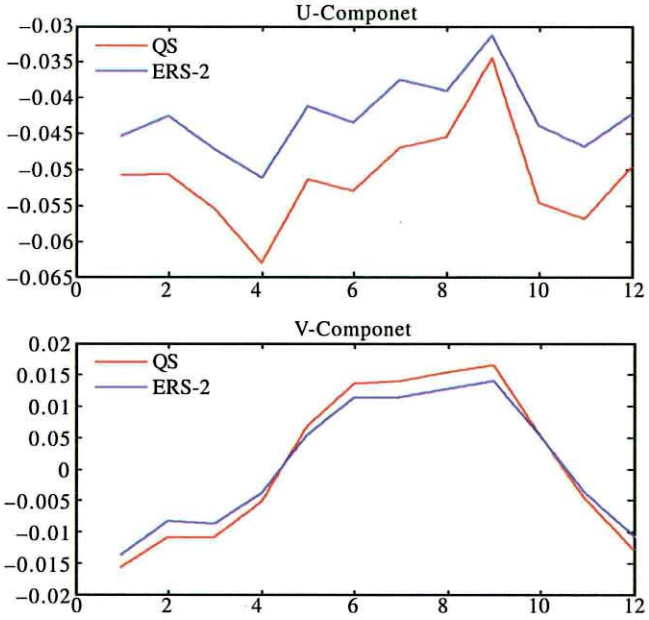

Figure 2. The averaged the wind stress in u- (upper) and v-components (bottom) in the study area during the overlap period of ERS-2 and QuikSCAT from January to December 2000

than those derived from QuikSCAT. This indicates that the VEOF result of the amplitude of wind stress increasing from 1999 is caused by the sensor difference, not the natural phenomenon. In order to have a longer time series of consistent wind data, linear regressions were applied to ERS data in u- and v-components, respectively to fit the QuikSCAT data from January to December 2000. Wind stress with more consistent magnitudes between ERS-2 and QuikSCAT are obtained and shown in Figure 3. We further applied the linear regressions in u- and v-components, respectively to the whole ERS dataset to generate a new dataset of wind stress from January 1993 to August 2007. This new dataset is analyzed by the VEOF method again.

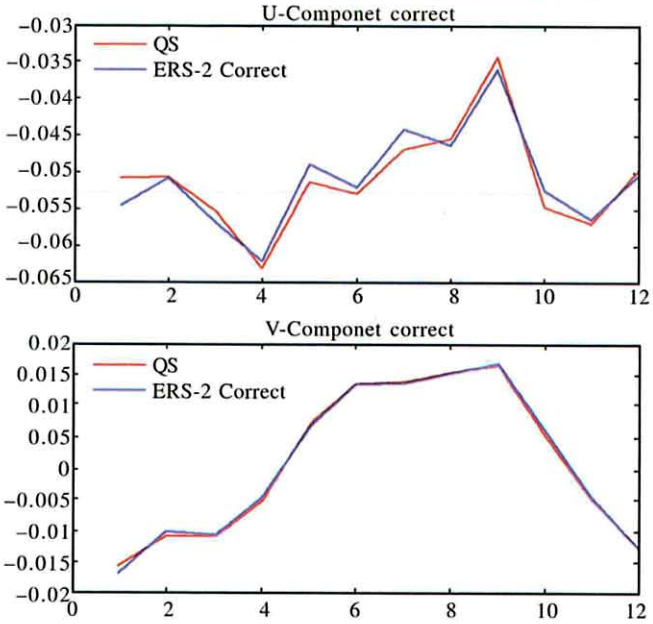

Figure 3. Same as Figure 2, but fitting of ERS-2 wind stress to QuikSCAT with linear regression functions

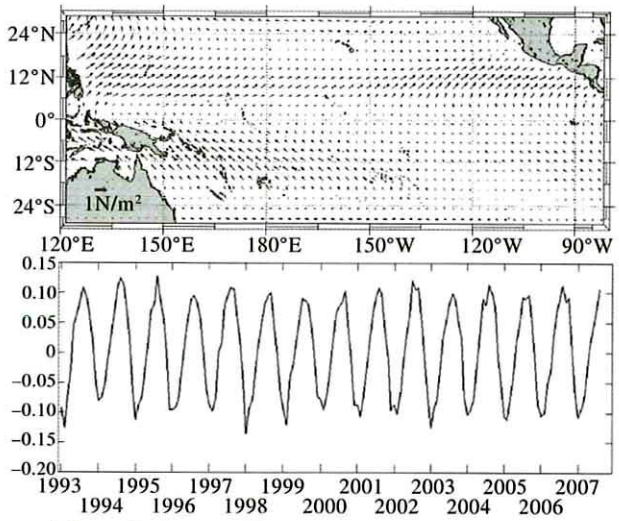

Figure 5. Same as Figure 4, but for the second VEOF

B. VEOF

The first VEOF mode (VEOF1) contains 69.6% of the variance of the data and primarily represents the trade winds, as shown in Figure 4. The temporal mode of VEOF1 is positive, implying that the wind directions in the spatial mode are unchanged. In the northern hemisphere, stronger trade winds are in the central tropical Pacific. However, in the southern hemisphere, stronger trade winds are in the western and eastern tropical Pacific. Near the equator, there is a calm zone in the western Pacific. The second VEOF mode (VEOF2) as shown in Figure 5, which accounts for 12.2% of the total variance, is characterized by an annual oscillation with positive and negative in boreal summer and winter, respectively. The spatial mode of VEOF2 is characterized by the southwesterly winds over the north-western tropical Pacific and along 6°–12°N, as well as the southeasterly winds over the south-western tropical Pacific near Australia. In boreal winter, the temporal mode of VEOF2 becomes negative, implying that the wind directions in the spatial mode reverse.

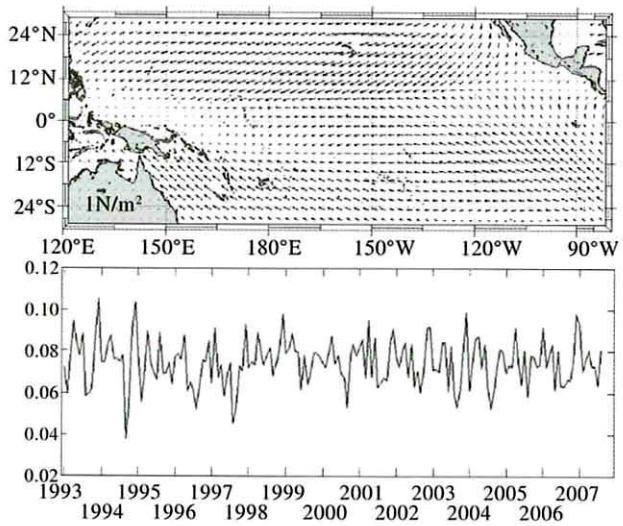

Figure 4. Same as Figure 1, but with adjustment of ERS-1/2 dataset

C. Anomaly EOF

In order to emphasize the interannual variability, the annual signal was filtered out from the wind stress dataset by calculating the climatological monthly means from January to December. The VEOF was applied to the residual wind stress data again. These VEOFs which are named anomaly VEOFs reveal the interannual variability of wind fields. The first anomaly VEOF(Figure 6) accounts for 19.8% of the anomaly variance. The temporal mode shows the maximum negative amplitude in the beginning of 1998 and the maximum positive amplitude in the beginning of 1999. Niño3.4 index is plotted on Figure 6, together with the temporal mode. One can see that the two curves are in good agreement. Furthermore, by applying cross-correlation analysis to both time series, the result shows that the correlation coefficient attains to maximum 0.9 with no time leg. In other words, it suggests that the

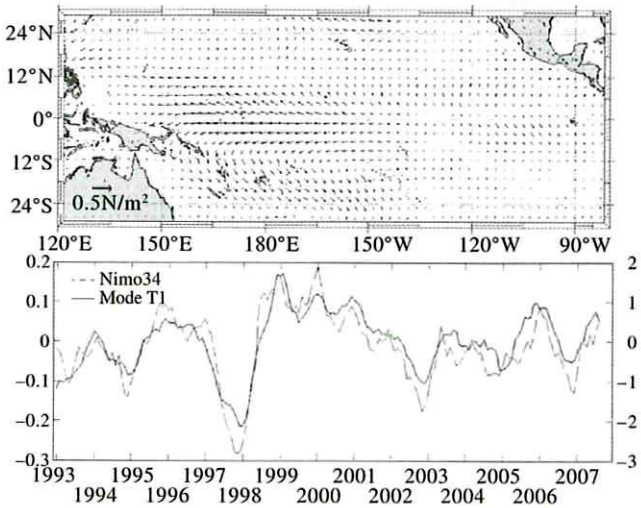

Figure 6. (a) The first anomaly VEOF spatial mode, (b) temporal mode (solid line) and Niño3.4 Index (dash line)

temporal mode which reflects interannual variability of winds in the tropical Pacific was almost in phase with variability of ENSO index. The result suggests not only the tight relationship between variations of winds in the tropical Pacific and ENSO events but also the significance of wind fields to dynamic of tropical Pacific. However, to deeply understand dynamical mechanism between tropical wind fields and ENSO events, further investigations are required. Moreover, negative amplitude of temporal mode during the El Niño period indicates that a strong westerly wind stress anomaly was in the western equatorial Pacific from 8°N to 8°S and from 150°E to 150°W, as shown in spatial mode of Figure 6. The maximum negative value appeared in the beginning of 1998 when was the strongest El Niño period. During the La Niña period, positive amplitude of temporal mode indicates that a strong easterly wind stress anomaly occurred over the area.

The second anomaly VEOF mode (Figure 7) accounts for 16.1% of the anomaly variance. The temporal mode shows a sharp increase of amplitude from May 1997 to January 1998 when is the period from the onset of 1997–1998 El Niño to its maturity. This mode implies that the variation of wind stress happened prior to the 1997–1998 El Niño event. The spatial mode shows two opposite directions of wind stress in the equatorial Pacific. One is on the western side from 120°E to 170°E and the other is over the middle-east part from 160°W to 110°W. The easterly winds reversed over the western equatorial Pacific from three to six months before the maturity of El Niño event. A similar phenomenon is also shown in the southern tropics. During the El Niño period, the easterly trade winds recovered on the western side of the equator and southern tropics, but the westerly winds moved to the equatorial middle-east. This seems related to the migration of western warm pool water to the central equatorial Pacific.

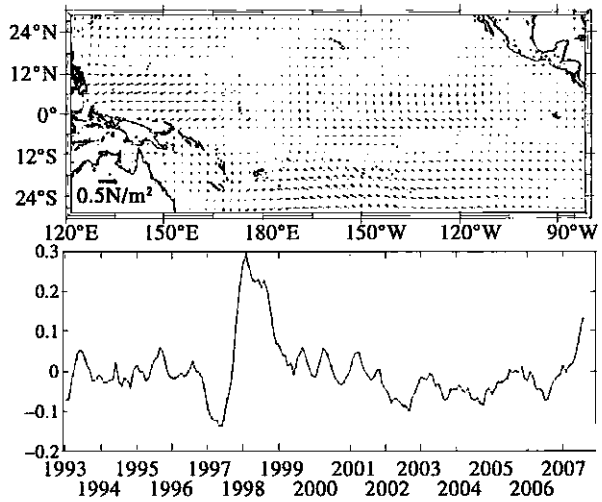

Figure 7. Same as Figure 6, but for the second mode

IV. SUMMARY

The data derived from ERS-1/2 and QuikSCAT scatterometers between 1993 and 2007 are used to study the variation of sea surface wind stress over the tropical Pacific Ocean. Since the magnitudes of wind stress derived from ERS-1/2 scatterometes are distinctly smaller than those derived from QuikSCAT during the overlap period, the magnitudes from ERS are adjusted to fit those derived from QuikSCAT. After correction of wind forcing, no wind stress trend is found from the dataset. The VEOF analysis is then applied to the wind stress dataset. The first VEOF mode reveals the variation of trade winds. The second VEOF mode indicates the seasonal variation which is related to the East Asia monsoon. After removing the climatological monthly mean from the wind stress dataset, the anomaly wind stress data shows highly correlated with El Niño/La Niña events.

ACKNOWLEDGEMENTS

We appreciate the French Research Institute for Exploitation of the Sea (IFREMER) for providing the wind stress data. This work was supported partially by the National Science Council of Taiwan under grants NSC 95-2611-M-019-008-MY3.

REFERENCES

[1] Lau K. M., Ding Y. H., Wang J. T., 2000, A report of the field operations and early results of the South China Sea Monsoon Experiment (SCSMEX). *Bull. Amer. Meteorol. Soc.* 81: 1261–1270.

[2] Lau K. M., Li X. F., Wu H. T., 2002, Evolution of the large scale circulation, cloud structure and regional water cycle associated with the South China Sea monsoon during May-June 1998. *J. Meteorol. Soc.* 80: 1129–1147.

[3] Huang R. H., Zhang R. H., Zhang Q. Y., 2002, The 1997/1998 ENSO cycle and its impact on summer climate anomalies in East Asia. *Adv. Atmos. Sci.* 17: 348–362.

[4] Zhu C. W., Nakazawa T., Li J. P., 2003, The 30–60 day intraseasonal oscillation over the western North Pacific Ocean and its impacts on summer flooding in China during 1998. *Geophys. Res. Lett.* 30: 1952, doi:10.1029/2003GL 017817.

[5] Qian J. H., Tao W. K., Lau K. M., 2004, Mechanisms for torrential rain associated with the mei-yu development during SCSMEX 1998. *Mon. Weather Rev.* 132: 3–27.

[6] Kawamura R., 1998, A possible mechanism of the Asian summer monsoon-ENSO coupling. *J. Meteorol. Soc. Jpn.* 76: 1009–1027.

[7] Pan J., Yan X. H., Zheng Q., 2003, Interpretation of scatterometer ocean surface wind vector EOFs over the Northwestern Pacific. *Remote Sens. Environ.* 84: 53–68.

[8] Inoue M., Bigg G. R., 1995, Trends in wind and sea-level pressure in the tropical Pacific Ocean for the period 1950–1979. *Int. J. Climatol.* 15: 35–52.

[9] Clarke A. J., Lebedev A., 1996, Long-term changes in the equatorial Pacific trade winds. *J. Clim.* 9: 1020–1029.

[10] Lagerloef G. S. E., Berstein R. L., 1988, Empirical orthogonal function analysis of Advanced Very High Resolution Radiometer surface temperature patterns in Santa Barbara Channel. *J. Geophys. Res.* 93: 6863–6873.

[11] Kelly K. A., 1988, Comments on "empirical orthogonal function analysis of advanced very high resolution radiometer surface patterns in Santa Barbara Channel". In G. S. E. Lagerloef, & R. L. Bernstein. *J. Geophys. Res.* 93: 15753–15754.

[12] Hardy D. M., Walton J. J., 1978, Principal component analysis of vector wind measurements. *J. Applied Meteorol.* 17: 1153–1162.